Rapid Fickian Yet Non-Gaussian Diffusion after Subdiffusion

Raffaele Pastore,[1,*] Antonio Ciarlo,[2] Giuseppe Pesce,[2] Francesco Greco,[1] and Antonio Sasso[2]
[1]Department of Chemical, Materials and Production Engineering, University of Naples Federico II, P.le Tecchio 80, Napoli 80125, Italy
[2]Department of Physics E. Pancini, University of Naples Federico II, Complesso Universitario Monte S. Angelo, Via Cintia, I-80126 Naples, Italy

(Received 2 January 2021; accepted 11 March 2021; published 12 April 2021)

The recently discovered Fickian yet non-Gaussian diffusion (FnGD) is here finely tuned and investigated over a wide range of probabilities and timescales using a quasi-2D suspension of colloidal beads under the action of a static and spatially random optical force field. This experimental model allows one to demonstrate that a "rapid" FnGD regime with a diffusivity close to that of free suspension can originate from earlier subdiffusion. We show that these two regimes are strictly tangled: as subdiffusion deepens upon increasing the optical force, deviations from Gaussianity in the FnGD regime become larger and more persistent in time. In addition, the distinctive exponential tails of FnGD are quickly built up in the subdiffusive regime. Our results shed new light on previous experimental observations and suggest that FnGD may generally be a memory effect of earlier subdiffusive processes.

DOI: 10.1103/PhysRevLett.126.158003

The hallmark of standard Brownian diffusion is twofold: the particle mean square displacement (MSD) increases linearly in time, which is also known as Fickian behavior, and the distribution of displacements is Gaussian. In fact, "Fickianity" and "Gaussianity" were thought to be strictly related since the time of Einstein's celebrated "random walk" description of Brownian motion. Seemingly, this relationship was more recently confirmed in other circumstances of thermal motion, generally known as anomalous diffusion [1–3], where an MSD that is nonlinearly increasing in time is typically accompanied by a non-Gaussian displacement distribution.

Around a decade ago, however, the discovery of Fickian yet non-Gaussian diffusion (FnGD) broke up such a well-established scenario [4]. Granick's group indeed found that colloidal tracers moving on phospholipid bilayer tubes and in actin gels display a linear MSD coexisting with a non-Gaussian displacement distribution [5]. Following these pioneer observations, several experiments identified FnGD in an increasing number of soft materials, including hard-sphere colloids [6], polymers on solid interfaces [7], nanospot systems [8,9], cells, and other active matter [10–14]. Further evidences of FnGD have been obtained by numerical simulations [15–17]. Such a wide variety of observations suggests that this phenomenon is quite ubiquitous in soft matter, although contrasting instances have also been provided [18]. (For soft materials, Gaussian but non-Fickian dynamics has also been reported [19,20].)

A few elegant models have been proposed to capture the main benchmarks of FnGD [21–31]. Many of these models share the idea of a "diffusing diffusivity," as introduced by Chubynsky and Slater [21]: the motion of a given particle is characterized by a varying diffusivity, either because the particle explores a heterogeneous but static structure of the matrix or because the matrix itself is evolving. The presence of some structural or dynamical heterogeneities of the environment seems indeed to be a a common feature of the wide variety of systems displaying FnGD. The multiplicity of relevant time and length scales arising from the heterogeneous nature of the environments makes experiments intrinsically challenging. The complex nature of the environment makes it difficult indeed to control its properties with high precision, and typically results in small ensembles of trajectories with durations typically limited to two decades in time. Conversely, large statistics and wide observation times would be required to sample the non-Gaussian tails [4] of the displacement distribution and to study both the short-time precursors and the long-time evolution of FnGD.

It so clearly appears that a finely controlled experimental model for an in-depth study of FnGD is on demand. Here we identify one such model: a very dilute monolayer of micron-sized hard-sphere colloids in water subjected to a weak, time-independent force field produced by a spatially stochastic distribution of optical intensities, also known as a speckle pattern [32]. Because of thermal fluctuations, tracers move in the static energy landscape generated by the speckle, which resembles popular theoretical models for heterogeneous diffusion [33,34]. A similar system was first introduced in a pioneering study that focused instead on a different range of control parameters with the aim of generating a subdiffusive, glassylike dynamics at intermediate times [35]. The Fickian regime, instead, was not fully attained over the observation time [35]. Other

 © 2021 American Physical Society

inspiring efforts, both numerical and experimental, then highlighted the tunability of this type of system [36,37].

In this Letter, we demonstrate that, with a judicious choice of the characteristic parameters, the considered system turns into an optimal experimental model for FnGD. We are indeed able to tune the "strength" and duration of FnGD finely by changing the optical power, and succeed in monitoring an unprecedented range of timescales and displacement probabilities. This opens the way to approach FnGD "from below" (i.e., from shorter times), looking for precursors, and to shed light on the long-time fate of this process. As a matter of fact, we find that FnGD occurs after a subdiffusive regime that takes place at shorter times; at the same time, we find that diffusivity is almost as large as in the free suspension (speckle-free conditions), a situation termed as "exceptionally rapid" by Granick's group [5].

In our setup, the static speckle is produced by a Spatial Light Modulator implemented with a digital mask, which allows highly reproducible realizations of the optical field as well as easy changes of its features. We perform experiments at different values of the optical power that controls the average intensity of the force field. The geometric properties of the patterns, determined by the digital mask, are instead kept fixed in all experiments. The quasi-2D nature of our systems makes it easy to track colloidal beads by standard digital videomicroscopy. For any given realization of the speckle, we can thus easily replicate the experiment several times to obtain a large number of long trajectories. [See the Supplemental Material (SM) [38] for details on methods and experimental setup.]

Figures 1(a) and 1(b) show two realizations of the speckle field: one "empty" and one with colloidal beads. The speckle pattern is characterized by intensity patches, also known as "grains." The typical grain size was set to $d_s \approx 4\ \mu$m, i.e., slightly larger than the bead diameter $d_p = 2.31\ \mu$m. We chose such a grain size on purpose to generate an environment akin to a soft matter matrix with heterogeneities comparable to the tracer size, which resembles, for instance, the conditions investigated in Ref. [5].

From an ensemble of hundreds of trajectories, we compute the MSD, $\Delta x^2(\Delta t) = \langle [x_i(t_0 + \Delta t) - x_i(t_0)]^2 \rangle_{i,t_0}$, and the probability distribution of particle displacement, $p(|\Delta x|, \Delta t) = \langle \delta(|\Delta x| - |x_i(t_0 + \Delta t) - x_i(t_0)|) \rangle_{i,t_0}$, where $\langle \rangle_{i,t_0}$ denotes averaging over trajectories and time origins [45].

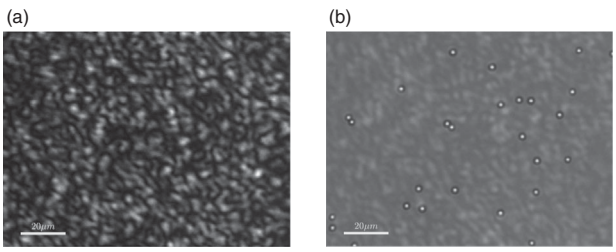

FIG. 1. At optical power $\Psi = 0.67$ W, (a) and (b) show two snapshots of the speckle field: "empty" and in the presence of the colloidal tracers, respectively.

We start by demonstrating that our model system clearly displays FnGD, focusing on the experiment at the largest optical power, $\Psi = 0.67$ W. Figure 2(a) shows indeed that, over the whole considered time span, the MSD displays a Fickian behavior, $\langle \Delta x^2(\Delta t) \rangle = 2D\Delta t$, where $D = 0.031\ \mu\text{m}^2\ \text{s}^{-1}$ is the diffusion coefficient. At any Δt within the time span of panel (a), however, the displacement distribution strongly deviates from the expected Gaussian $g(|\Delta x|, \Delta t) = \sqrt{(2/\pi \langle \Delta x^2(\Delta t) \rangle}\, \exp\left[-(\Delta x^2/2\langle \Delta x^2(\Delta t) \rangle\right]$ [46], as shown in Fig. 2(b), that reports, as an example, $p(|\Delta x|, \Delta t)$ for $\Delta t = 400$ s [distributions corresponding to other Δt in the same time span are shown in Fig. 3(c)]. An excess probability is apparent for very small and large displacements, whereas a defect probability is present in a range of intermediate displacements. In addition, the tail of the distribution reveals a clear exponential behavior consistent with Diffusing Diffusivity and other theoretical models for FnGD [21,22,30]. It is $p(|\Delta x|, \Delta t) \propto \exp[-|\Delta x|/\lambda(\Delta t)]$, where $\lambda(\Delta t)$ is a time-dependent decay length, as discussed below. Overall, there is an impressive similarity between the present results and those provided in the original paper by Granick's group [5]. In particular, we invite the reader to compare Fig. 2 to the data for the actin gel system reported in Figs. 3B and 3C of Ref. [5]. The only relevant difference is in the timescale, which is larger in our case. This is a trivial consequence of the fact that we have chosen to employ large tracers to facilitate monitoring the short-term dynamics. In contrast, in the experiments by Granick's group, the tracer radii were constrained to a range of tens of nanometers by the mesh size of the actin gel. Notice that, in order to fully appreciate the similarities with Figs. 3B and 3C of Ref. [5], we have limited the data in Fig. 2 to the same ranges achieved in that work, corresponding roughly to two decades in time and probability. As a

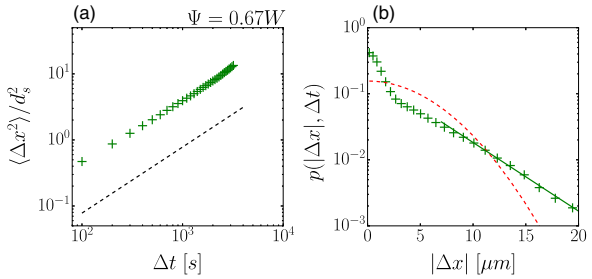

FIG. 2. At optical power $\Psi = 0.67$ W, (a) MSD normalized by the square grain size as a function time. The dashed line $\langle \Delta x^2 \rangle \propto t$ corresponds to a Fickian behavior. (b) Displacement distribution $p(|\Delta x|, \Delta t)$ for time $\Delta t = 400$ s. The dashed line corresponds to the Gaussian distribution for a standard Brownian motion. The data in both panels cover a limited portion of the investigated range.

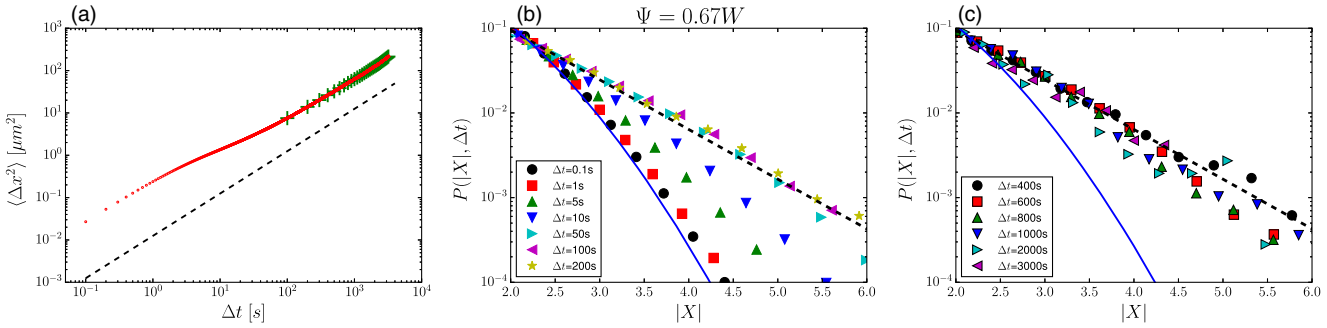

FIG. 3. At optical power $\Psi = 0.67$ W, (a) MSD over the whole investigated time span. For a direct comparison, the dataset of Fig. 2(a) is also reported (crosses). (b),(c) Distributions of particle displacements after performing the rescaling discussed in the text at different lag-times Δt within the time spans of the subdiffusive and FnGD regimes, respectively. The data cover the two decades in probability below those presented in Fig. 2(b). The universal Gaussian distribution $G(|X|)$ is reported as a continuous line. The dashed lines in both panels are the same exponential law $A \exp[-(|X|/\Lambda)]$ obtained by fit to the data at the Fickian time $\Delta t = t_f$.

matter of fact, we are able to explore much larger ranges, up to about 4.5 decades in time and four decades in probability.

Indeed, Fig. 3(a) shows the MSD for the overall investigated time window that corresponds to a much higher temporal resolution if compared to the data in Fig. 2. Hence, the nature of the early dynamics underlying FnGD is disclosed: at the very short time $\Delta t < 1s$, the data are compatible with a linear increase, $\langle \Delta x^2(\Delta t) \rangle \propto \Delta t$, but with a "short-time" diffusion coefficient roughly four times larger than the "long-time" one D. This regime can be understood as a free diffusion occurring on a length range much smaller than the characteristic grain size (up to $\Delta x_i^2 \simeq 300$ nm^2), where the optical gradient does not yet affect the particle motion. At the longer time $\Delta t > 1$ s, a moderate subdiffusive regime takes place, extending roughly over two decades in time, up to attaining the long-time Fickian diffusion. The observation of the recovery of Fickianity from the short-time side offers us the opportunity to quantitatively estimate the characteristic time of this process, t_f, which will correspond to the upper boundary of subdiffusion. For this experiment, we measure $t_f \simeq 400$ s using the approach described later in the text.

We now proceed to inspect the displacement distribution at different Δt within the overall observation time. To properly compare the distributions on such a wide range of timescales (and length scales), from now on we will rescale the axes as follows: $|\Delta x| \to |X| = (|\Delta x|/\sqrt{\langle \Delta x^2(\Delta t) \rangle})$, and $p(|\Delta x|, \Delta t) \to P(|X|, \Delta t) = p(|\Delta x|, \Delta t)\sqrt{\langle \Delta x^2(\Delta t) \rangle}$ to preserve normalization. Notice that, with this rescaling, the Gaussian distribution $g(|\Delta x|, \Delta t)$ corresponding to "pure" Brownian motion becomes a universal time-independent curve: $G(|X|) = \sqrt{2/\pi} e^{-(X^2/2)}$. Figures 3(b) and 3(c) show the tails of a number of these distributions, extending the range of probability of Fig. 2(b) by about two decades. In particular, Fig. 3(b) focuses on a range of Δt spanning the short-term and subdiffusive regimes observed in the MSD, whereas Fig. 3(c) refers to values of Δt from the onset of the Fickian regime t_f to the end of the observation time. At very short times, the data in panel (b) are consistent with the standard Gaussian, as expected for free diffusion. Entering the subdiffusive regime, progressive deviations from the Gaussian are observed. Well within the subdiffusive time window, the data seems to "saturate" to a robust exponential decay over the whole probability range considered (three decades), $P(|X|, \Delta t) \simeq A e^{-(|X|/\Lambda)}$, where Λ is a nondimensional decay length. Remarkably, panel (c) shows that such an exponential behavior fully persists in the Fickian regime, up to the largest observation time, with essentially the same time-independent decay length Λ observed in the late subdiffusive regime. This reveals that the distinctive tails characterizing FnGD are already fully built during the preceding subdiffusion without any clear sign of breakup of the exponential behavior or any other type of time evolution, at least over the duration of this experiment.

Concerning panels (b) and (c), notice that the existence of a time-independent, nondimensional decay length Λ corresponds to a dimensional decay length λ scaling as the square root of time, which represents another analogy between our experiments and the results of Granick's group [5,6]. Indeed, going back to the original variables, one finds that $\lambda(\Delta t) = \Lambda\sqrt{2D\Delta t}$.

We now show how our experimental setup readily enables for tuning the "strength" of FnGD to unveil other features of this phenomenon. Figure 4(a) displays all MSDs, including two lower optical intensities, $\Psi = 0.43$ W and 0.61 W, and the speckle-free case ($\Psi = 0$). All the MSDs share a unique short-time linear behavior characterized by the same diffusivity as the speckle-free diffusion, once again confirming that this early regime is a standard free diffusion. For the intermediate time $\Delta t > 1$ s, subdiffusion is always present at finite optical power but is more marked at larger Ψ. Then, Fickian diffusion is restored at long times.

To better appreciate these features, Fig. 4(b) shows the logarithmic derivative $u(\Delta t) = (d \log \langle \Delta x^2(\Delta t) \rangle / d \log \Delta t)$

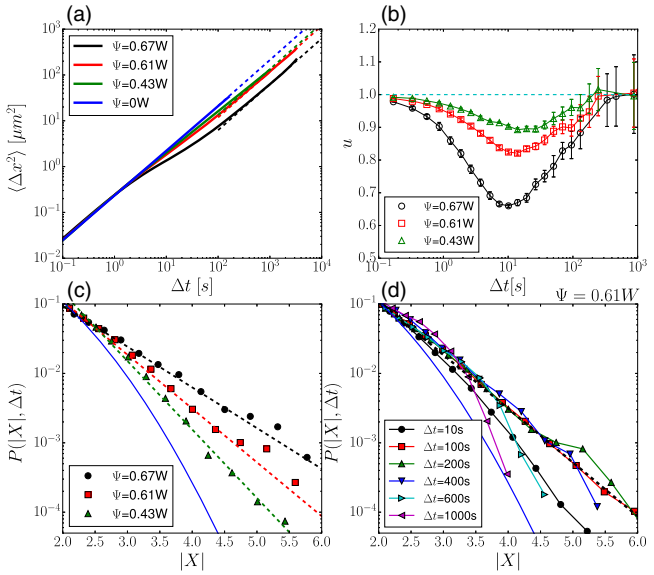

FIG. 4. (a) MSD and (b) its logarithmic derivative $u(\Delta t) = (d \log \langle \Delta x^2(\Delta t) \rangle / d \log \Delta t)$ as a function of time for the different optical powers Ψ, as indicated. The dashed lines are fits to the long-time Fickian regime $\langle \Delta x^2(\Delta t) \rangle = 2D\Delta t$, with diffusivities $D = 0.031,\ 0.059,\ 0.066,\ 0.106\ \mu\text{m}^2\,\text{s}^{-1}$ for $\Psi = 0.67,\ 0.61,\ 0.43,\ 0$ W, respectively. Tails of the distributions of particle displacements after performing the rescaling discussed in the text, (c), at lag-time $\Delta t = t_f(\Psi)$ and for different optical powers Ψ and (d) for the intermediate optical power $\Psi = 0.61$ W and different times Δt ranging in the subdiffusive and FnGD regimes. In both panels (c) and (d), the universal Gaussian distribution $G(|X|)$ is reported as a continuous line. The dashed lines are exponentials $A \exp[-(|X|/\Lambda)]$ obtained by fitting the tails of $P(|X|, \Delta t = t_f)$ at the different powers.

in the time span 10^{-1}–10^3 s, which provides an estimate of the local slope of the MSDs in panel (a). In agreement with the just presented MSD behavior, $u(\Delta t)$ is consistent with unity for short and long times and is instead smaller than unity for intermediate times. The presence of a more pronounced minimum at larger optical power clearly indicates a "deeper" subdiffusion. On increasing the optical power, the duration of the subdiffusive regime (the time span where $u < 1$) and, in turn, the time for restoring the long-time Fickian diffusion also increase. By monitoring when $u(\Delta t)$ first becomes consistent with unity, we estimate the Fickian time $t_f \simeq 150,\ 200,\ 400$ s for $\Psi = 0.43,\ 0.61,\ 0.67$ W, respectively.

Panel (a) also shows that, in the long-time Fickian regime, changing the optical power leads to a variation of the diffusion coefficient: on increasing the power, we find a roughly fourfold reduction of D with respect to the speckle-free value. A comparable, relatively small reduction of the diffusivity was observed for the phospholipid tube system of Ref. [5,6], and the dynamics of that system was therefore called "exceptionally rapid." In this sense, we are therefore also dealing with "exceptionally rapid" dynamics, even at our strongest optical power. Our results, however, clarify that such a "rapid dynamics" can occur after a subdiffusive-crossover regime (commonly associated with slow dynamics, i.e., in glass-forming liquids).

We now move on to consider how $P(|X|, \Delta t)$ changes on varying the optical power. Figure 4(c) compares the tails of $P(|X|, \Delta t)$ at the onset of the Fickian regime $\Delta t = t_f(\Psi)$ for the three investigated powers. The distributions display a clear-cut exponential behavior even at the smallest optical power, demonstrating that FnGD is always clearly manifested in our experiments. The nondimensional decay length, however, appears to grow on enhancing the power: precisely, Λ is found to be 0.44 and 0.74 at the smallest and largest powers, respectively. (Notice that a constant Λ would be implied by a pure exponential distribution in a Fickian regime.) Figure 4(d) shows the tails of the distributions at the intermediate optical power $\Psi = 0.61$ W for different Δt. The trend at a not-too-large time ($\Delta t \lesssim 400$ s) is qualitatively similar to the one already presented for the strongest optical power: robust exponential tails are already built in the subdiffusive regime and persist for a while in the Fickian regime, with the decay length Λ being essentially time-independent. However, a major difference with the experiments at the largest power emerges at long times: close to the edge of the observation time, in fact, it is possible to appreciate deviations from the exponential behavior, with a tendency to revert toward the Gaussian distribution, in agreement with the long-time prediction of Diffusing Diffusivity [21]. The data at the smallest optical power are qualitatively similar, with the exponential behavior being even less persistent. On the other hand, the seemingly "frozen" exponential decay at the highest power [see Fig. 3(c)] can now be understood in terms of a time for restoring Gaussianity that is much larger than the experimental timescale. While longer-lasting experiments would be needed to quantitatively measure a characteristic time for Gaussian recovery, it is quite clear that, on increasing the optical power, not only the strength but also the duration of the FnGD regime increase.

Conclusions.—In this Letter, we succeed in generating FnGD by using a quasi-2D dilute colloidal suspension and exploiting a static random optical field as a proxy of a soft matter environment. FnGD is found to be closely tangled with a temporary subdiffusion occurring at a shorter time, up to two time decades earlier. In fact, the non-Gaussian deviations characterizing FnGD are already fully built during the preceding subdiffusion, and their magnitude and duration increase as the subdiffusion becomes more marked and lasts longer. Remarkably, such a subdiffusive regime yet leads to an "impressively rapid" Fickian dynamics. A short-time subdiffusion and an impressively rapid Fickian diffusion were separately observed by Granick's group [5]. Some of the actin gel systems display signs of subdiffusion followed by relatively slow Fickian diffusion and no observable tendency to Gaussian recovery. The phospholipid tube systems, in contrast, always show

rapid Fickian diffusion with no hints of subdiffusion at short times and a clear tendency to Gaussian recovery at the longest time. Notice that roughly the same temporal resolution was adopted in the experiments by Granick's group for the two systems. It is thus likely that a subdiffusive regime would exist also for the phospholipid tube systems but occurring below the temporal resolution of those experiments. Our own experiments support this possibility by showing that, as the time for recovering Gaussianity decreases, the upper boundary of subdiffusion also shifts to shorter times. Thus, the presence of short-time subdiffusion may be a general precursor of FnGD rather than a specific feature of our model system: indeed, subdiffusion and FnGD are expected to share a common origin in system heterogeneities. In this sense, the observation of seemingly different behaviors may have a merely quantitative rather than a qualitative origin. In many experimental situations, indeed, the subdiffusive regime (and the associated activation events) may occur on timescales too small to be detected.

As for perspectives, insights may be provided by measuring the statistics of residence times [47,48] or of a properly defined single-particle diffusivity, which should allow for comparison to Continuous Time Random Walk or Diffusing Diffusivity ideas [21,22,30]. It would also be interesting to perform experiments by varying the speckle grain size or using time-dependent speckle patterns to mimic an environment evolving in time.

We acknowledge Flavio Seno for useful and inspiring discussions.

*Corresponding author.
raffaele.pastore@unina.it

[1] Y. Meroz and I. M. Sokolov, A toolbox for determining subdiffusive mechanisms, Phys. Rep. **573**, 1 (2015).
[2] J.-P. Bouchaud and A. Georges, Anomalous diffusion in disordered media: Statistical mechanisms, models and physical applications, Phys. Rep. **195**, 127 (1990).
[3] R. Metzler and J. Klafter, The random walk's guide to anomalous diffusion: A fractional dynamics approach, Phys. Rep. **339**, 1 (2000).
[4] B. Wang, J. Kuo, S. C. Bae, and S. Granick, When Brownian diffusion is not Gaussian, Nat. Mater. **11**, 481 (2012).
[5] B. Wang, S. M. Anthony, S. C. Bae, and S. Granick, Anomalous yet Brownian, Proc. Natl. Acad. Sci. U.S.A. **106**, 15160 (2009).
[6] J. Guan, B. Wang, and S. Granick, Even hard-sphere colloidal suspensions display fickian yet non-gaussian diffusion, ACS Nano **8**, 3331 (2014).
[7] C. Yu, J. Guan, K. Chen, S. C. Bae, and S. Granick, Single-molecule observation of long jumps in polymer adsorption, ACS Nano **7**, 9735 (2013).
[8] K. He, F. Babaye Khorasani, S. T. Retterer, D. K. Thomas, J. C. Conrad, and R. Krishnamoorti, Diffusive dynamics of nanoparticles in arrays of nanoposts, ACS Nano **7**, 5122 (2013).
[9] K. He, S. T. Retterer, B. R. Srijanto, J. C. Conrad, and R. Krishnamoorti, Transport and dispersion of nanoparticles in periodic nanopost arrays, ACS Nano **8**, 4221 (2014).
[10] W. He, H. Song, Y. Su, L. Geng, B. J. Ackerson, H. Peng, and P. Tong, Dynamic heterogeneity and non-Gaussian statistics for acetylcholine receptors on live cell membrane, Nat. Commun. **7**, 11701 (2016).
[11] T. Kwon, O.-S. Kwon, H.-J. Cha, and B. J. Sung, Stochastic and heterogeneous cancer cell migration: experiment and theory, Sci. Rep. **9**, 16927 (2019).
[12] K. C. Leptos, J. S. Guasto, J. P. Gollub, A. I. Pesci, and R. E. Goldstein, Dynamics of Enhanced Tracer Diffusion in Suspensions of Swimming Eukaryotic Microorganisms, Phys. Rev. Lett. **103**, 198103 (2009).
[13] H. Kurtuldu, J. S. Guasto, K. A. Johnson, and J. P. Gollub, Enhancement of biomixing by swimming algal cells in two-dimensional films, Proc. Natl. Acad. Sci. U.S.A. **108**, 10391 (2011).
[14] R. Jeanneret, D. O. Pushkin, V. Kantsler, and M. Polin, Entrainment dominates the interaction of microalgae with micron-sized objects, Nat. Commun. **7**, 12518 (2016).
[15] J. T. Kalathi, U. Yamamoto, K. S. Schweizer, G. S. Grest, and S. K. Kumar, Nanoparticle Diffusion in Polymer Nanocomposites, Phys. Rev. Lett. **112**, 108301 (2014).
[16] J. Kim, C. Kim, and B. J. Sung, Simulation Study of Seemingly Fickian but Heterogeneous Dynamics of Two Dimensional Colloids, Phys. Rev. Lett. **110**, 047801 (2013).
[17] S. Acharya, U. K. Nandi, and S. Maitra Bhattacharyya, Fickian yet non-Gaussian behaviour: A dominant role of the intermittent dynamics, J. Chem. Phys. **146**, 134504 (2017).
[18] A. Cuetos, N. Morillo, and A. Patti, Fickian yet non-Gaussian diffusion is not ubiquitous in soft matter, Phys. Rev. E **98**, 042129 (2018).
[19] R. Poling-Skutvik, R. Krishnamoorti, and J. C. Conrad, Size-dependent dynamics of nanoparticles in unentangled polyelectrolyte solutions, ACS Macro Lett. **4**, 1169 (2015).
[20] T. K. Piskorz and A. Ochab-Marcinek, A universal model of restricted diffusion for fluorescence correlation spectroscopy, J. Phys. Chem. B **118**, 4906 (2014).
[21] M. V. Chubynsky and G. W. Slater, Diffusing Diffusivity: A Model for Anomalous, yet Brownian, Diffusion, Phys. Rev. Lett. **113**, 098302 (2014).
[22] A. V. Chechkin, F. Seno, R. Metzler, and I. M. Sokolov, Brownian yet Non-Gaussian Diffusion: From Superstatistics to Subordination of Diffusing Diffusivities, Phys. Rev. X **7**, 021002 (2017).
[23] J. Slezak, R. Metzler, and M. Magdziarz, Superstatistical generalised Langevin equation: non-Gaussian viscoelastic anomalous diffusion, New J. Phys. **20**, 023026 (2018).
[24] R. Jain and K. Sebastian, Lévy flight with absorption: A model for diffusing diffusivity with long tails, Phys. Rev. E **95**, 032135 (2017).
[25] V. Sposini, D. S. Grebenkov, R. Metzler, G. Oshanin, and F. Seno, Universal spectral features of different classes of random-diffusivity processes, New J. Phys. **22**, 063056 (2020).

[26] R. Jain and K. Sebastian, Diffusing diffusivity: a new derivation and comparison with simulations, J. Chem. Sci. **129**, 929 (2017).
[27] Y. Lanoiselée, N. Moutal, and D. S. Grebenkov, Diffusion-limited reactions in dynamic heterogeneous media, Nat. Commun. **9**, 4398 (2018).
[28] Y. Lanoiselée and D. S. Grebenkov, A model of non-Gaussian diffusion in heterogeneous media, J. Phys. A **51**, 145602 (2018).
[29] Y. Hachiya, T. Uneyama, T. Kaneko, and T. Akimoto, Unveiling diffusive states from center-of-mass trajectories in glassy dynamics, J. Chem. Phys. **151**, 034502 (2019).
[30] E. Barkai and S. Burov, Packets of Diffusing Particles Exhibit Universal Exponential Tails, Phys. Rev. Lett. **124**, 060603 (2020).
[31] S. Mora and Y. Pomeau, Brownian diffusion in a dilute field of traps is Fickean but non-Gaussian, Phys. Rev. E **98**, 040101 (2018).
[32] J. W. Goodman, *Speckle Phenomena in Optics: Theory and Applications* (Roberts and Company Publishers, Greenwood Village, CO, 2007).
[33] R. Zwanzig, Diffusion in a rough potential, Proc. Natl. Acad. Sci. U.S.A. **85**, 2029 (1988).
[34] M. Schmiedeberg, J. Roth, and H. Stark, Brownian particles in random and quasicrystalline potentials: How they approach the equilibrium, Eur. Phys. J. E **24**, 367 (2007).
[35] F. Evers, C. Zunke, R. D. Hanes, J. Bewerunge, I. Ladadwa, A. Heuer, and S. U. Egelhaaf, Particle dynamics in two-dimensional random-energy landscapes: Experiments and simulations, Phys. Rev. E **88**, 022125 (2013).
[36] G. Volpe, G. Volpe, and S. Gigan, Brownian motion in a speckle light field: Tunable anomalous diffusion and selective optical manipulation, Sci. Rep. **4**, 3936 (2014).
[37] G. Volpe, L. Kurz, A. Callegari, G. Volpe, and S. Gigan, Speckle optical tweezers: micromanipulation with random light fields, Opt. Express **22**, 18159 (2014).
[38] See Supplemental Material, which includes Refs. [39–44], at http://link.aps.org/supplemental/10.1103/PhysRevLett.126.158003 for details on the experiments.
[39] G. Pesce, G. Volpe, O. M. Maragó, P. H. Jones, S. Gigan, A. Sasso, and G. Volpe, Step-by-step guide to the realization of advanced optical tweezers, J. Opt. Soc. Am. B **32**, B84 (2015).
[40] P. H. Jones, O. M. Maragò, and G. Volpe, *Optical Tweezers: Principles and Applications* (Cambridge University Press, Cambridge, England, 2015).
[41] J. Dainty, *Progress in Optics XIV*, edited by E. Wolf (North-Holland, Amsterdam, 1976).
[42] B. Zhang, J. Zerubia, and J.-C. Olivo-Marin, Gaussian approximations of fluorescence microscope point-spread function models, Appl. Opt. **46**, 1819 (2007).
[43] J. C. Crocker and D. G. Grier, Methods of digital video microscopy for colloidal studies, J. Colloid Interface Sci. **179**, 298 (1996).
[44] I. F. Sbalzarini and P. Koumoutsakos, Feature point tracking and trajectory analysis for video imaging in cell biology, J. Struct. Biol. **151**, 182 (2005).
[45] We also average over both the x and y coordinates of each particle since the system is isotropic. Of course, we checked that the displacements along x and y, both negative and positive, lead to the same distributions within the statistical noise.
[46] Like for the other distributions, we adopted the normalization $\int_0^\infty g(|\Delta x|, \Delta t)dx = 1$.
[47] P. Chaudhuri, L. Berthier, and W. Kob, Universal Nature of Particle Displacements close to Glass and Jamming Transitions, Phys. Rev. Lett. **99**, 060604 (2007).
[48] J. Helfferich, F. Ziebert, S. Frey, H. Meyer, J. Farago, A. Blumen, and J. Baschnagel, Continuous-time random-walk approach to supercooled liquids. I. Different definitions of particle jumps and their consequences, Phys. Rev. E **89**, 042603 (2014).